Fakultät für Physik
Institut für Theorie der Kondensierten Materie

Another thesis on SNS junctions: numerical simulations and calculations

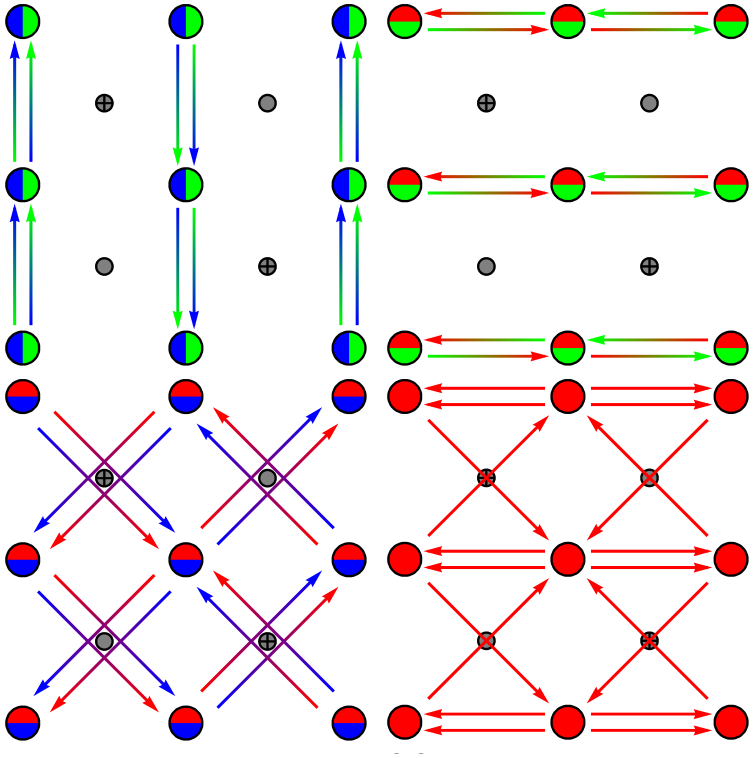

Master's Thesis
by
Umut Nefta Kanilmaz
Submission date: 25. February 2018

Advisor: PD Dr. Igor Gornyi
Co-Advisor: Prof. Dr. Alexander Mirlin

Ich erkläre hiermit, dass die Arbeit selbstständig angefertigt, alle benutzten Quellen und Hilfsmittel vollständig und genau angegeben und alles kenntlich gemacht wurde, das aus Arbeiten anderer unverändert oder mit Abänderungen entnommen ist.

Karlsruhe, den 24. Januar 2017

. . . . . .
(**Alexander Gawrilow**)

Contents

1 Framework for analytical model

1.1 Theory of superconductivity

The discovery of the isotope effect in 1950 revealed that not only lattice electrons but rather the whole lattice determines the superconducting properties of a solid. Experiments measuring the critical temperature T_c of different mercury isotopes showed that indeed, there is a relation between the isotope mass and T_c. Herbert Frölich was then the first to introduce a new concept to explain superconductivity. He showed that a phonon-intermediated interaction between electrons and the lattice could lead to an attractive long-range interaction of electrons in the lattice. Figuratively speaking, an electron passing through the crystal lattice will polarize it by attracting the positive ions. It leaves a deformed lattice, which will then attract a second electron. An effective attractive interaction between these two electrons is created. In 1956, Cooper showed that the electronic ground state, the Fermi sea at $T = 0$, is unstable if a weak attractive interaction is taken into account. This layed the foundation of the BCS theory [1], the first microscopic theory after the discovery in 1911 by Heike Kammerlingh Onnes.

This is the first paper with Superconductivity

Formulas needed

Hamiltonian:

$$H = H_0 + H_1 \tag{1.1}$$

$$H_0 = \sum_{\mathbf{k},\sigma} \xi_{\mathbf{k}} c^\dagger_{\mathbf{k}\sigma} c_{\mathbf{k}\sigma} \tag{1.2}$$

$$H_1 = \frac{1}{N} \sum_{\mathbf{k},\mathbf{k}'} V_{\mathbf{k},\mathbf{k}'} c^\dagger_{\mathbf{k}\uparrow} c^\dagger_{-\mathbf{k}\downarrow} c_{-\mathbf{k}'\downarrow} c_{\mathbf{k}'\uparrow} \tag{1.3}$$

The operators $c^\dagger_{\mathbf{k},\sigma}, c_{\mathbf{k},\sigma}$ are fermion operators that create or annihilate an electron with momentum $\mathbf{k}$ and spin σ. The first term in the Hamiltonian H is the unperturbed electron Hamiltonian H_0 with parabolic energy dispersion $\xi_{\mathbf{k}}$. The second term is the interaction Hamiltonian H_1, expressing the scattering of two electrons from $(-\mathbf{k}' \downarrow, \mathbf{k}' \uparrow)$ to $(\mathbf{k} \uparrow, -\mathbf{k} \downarrow)$. The interaction potential $V_{\mathbf{k},\mathbf{k}'}$ exchanges the scattering for electrons with energy $|\xi_{\mathbf{k}}| \lesssim \hbar\omega_D$. The Hamiltonian in eq. (1.1) can be simplified by doing a mean-field approximation. In this approximation, an operator A is expressed by a sum of its statistical mean $\langle A \rangle$ and small statistical fluctuations δA. Since the fluctuations

are assumed to be small, terms with $\mathcal{O}((\delta A)^2)$ can be neglected.

$$\begin{aligned} A &= \langle A\rangle + \delta A, \quad B = \langle B\rangle + \delta B \\ AB &= \langle A\rangle\langle B\rangle + \langle A\rangle\delta B + \langle B\rangle\delta A + \underbrace{\delta A \delta B}_{\approx 0} \end{aligned} \tag{1.4}$$

Using $\delta A = A - \langle A\rangle$ and inserting this back into eq. (1.4) leads to

$$AB = \langle A\rangle B + \langle B\rangle A - \langle A\rangle\langle B\rangle. \tag{1.5}$$

This approximation is applied to the interaction part H_1 in eq. (1.3), replacing

$$A = c^\dagger_{\mathbf{k}\uparrow} c^\dagger_{-\mathbf{k}\downarrow}, \quad B = c_{-\mathbf{k}'\downarrow} c_{\mathbf{k}'\uparrow}. \tag{1.6}$$

The result is the BCS-Hamiltonian

$$H_{\mathrm{BCS}} = \sum_{\mathbf{k},\sigma} \xi_{\mathbf{k}} c^\dagger_{\mathbf{k}\sigma} c_{\mathbf{k}\sigma} - \sum_{\mathbf{k}} \Delta^*_{\mathbf{k}} c_{-\mathbf{k},\downarrow} c_{\mathbf{k},\uparrow} - \sum_{\mathbf{k}} \Delta_{\mathbf{k}} c^\dagger_{\mathbf{k}\uparrow} c^\dagger_{-\mathbf{k}\downarrow} + \text{const.} \tag{1.7}$$

where

$$\Delta_{\mathbf{k}} := -\frac{1}{N} \sum_{\mathbf{k}'} V_{\mathbf{k}\mathbf{k}'} \langle c_{-\mathbf{k}',\downarrow} c_{\mathbf{k}'\uparrow}\rangle \tag{1.8}$$

$$\Delta^*_{\mathbf{k}} := -\frac{1}{N} \sum_{\mathbf{k}'} V_{\mathbf{k},\mathbf{k}'} \langle c^\dagger_{\mathbf{k}'\uparrow} c^\dagger_{-\mathbf{k}'\downarrow}\rangle \tag{1.9}$$

The BCS-Hamiltonian in eq. (1.7) can be diagonalized using the Bogoliubov transformation. The aim is to express the Hamiltonian in the basis of new fermion operators. These new operators will describe quasiparticles, which are a linear combination of $c^\dagger_{\mathbf{k},\sigma}$ and $c_{\mathbf{k},\sigma}$.

$$\begin{pmatrix} \gamma_{\mathbf{k}\uparrow} \\ \gamma^\dagger_{-\mathbf{k}\downarrow} \end{pmatrix} = \begin{pmatrix} u^*_{\mathbf{k}} & -v_{\mathbf{k}} \\ v^*_{\mathbf{k}} & u_{\mathbf{k}} \end{pmatrix} \begin{pmatrix} c_{\mathbf{k}\uparrow} \\ c^\dagger_{-\mathbf{k}\downarrow} \end{pmatrix} \tag{1.10}$$

Evaluating the fermion anticommutation relation using the transformation above yields

$$\left\{\gamma_{\mathbf{k}\uparrow}, \gamma^\dagger_{\mathbf{k}\uparrow}\right\} = \cdots = |u_{\mathbf{k}}|^2| + v_{\mathbf{k}}|^2 \stackrel{!}{=} 1 \tag{1.11}$$

and will lead to the inverse transformation of eq. (1.1). Inserting the inverse transformation into the BCS-Hamiltonian in eq.(1.7) will give the coefficients $u_{\mathbf{k}}$, $v_{\mathbf{k}}$ from eq. (1.1) and finally yield to the diagonalized form of the BCS-Hamiltonian

$$H_{\mathrm{BCS}} = \sum_{\mathbf{k}\sigma} E_{\mathbf{k}} \gamma^\dagger_{\mathbf{k}\sigma} \gamma_{\mathbf{k}\sigma} \tag{1.12}$$

$$E_{\mathbf{k}} := \sqrt{\xi^2_{\mathbf{k}} + |\Delta_{\mathbf{k}}|^2} \tag{1.13}$$

interpretation as holes, etc
plots of particle and hole exitation (dispersion relation with gap)
metion fermi surface and so on

Bogoliubov de Gennes Hamiltonian

The ansatz for the BCS ground state used by Bardeen, Cooper and Schrieffer is based on the concept of Cooper pairs. It is a direct consequence of the instability in the ground state through the attractive interaction. The BCS theory proposes a BCS ground state built on eigenstates of the single-particle Hamiltonian H_0 from eq. (1.2), leading to a ground state that consists of a linear combination of pair states.

$$\left|\psi_{\mathrm{BCS}}\right\rangle = \prod_{\mathbf{k}} (u_{\mathbf{k}} + v_{\mathbf{k}} c^{\dagger}_{\mathbf{k}\uparrow} c^{\dagger}_{-\mathbf{k}\downarrow}) \left|\mathrm{vac}\right\rangle \tag{1.14}$$

$$H_{\mathrm{BCS}} \left|\psi_{\mathrm{BCS}}\right\rangle = E_{\mathrm{BCS}} \left|\psi_{\mathrm{BCS}}\right\rangle \tag{1.15}$$

In most cases however, a more realistic set-up or inhomogeneous system cannot be described in terms of eigenfunctions of H_0. With a vector potential $\mathbf{A} \neq 0$, for example, time reversal symmetry is not given any more. The characteristic length scale is the superconducting coherence length ξ_0. If a system is varying slowly over a length scale $l \approx \xi_0$, a spatially dependent, more general Hamiltonian is needed. In order to find an adequate expression for such a spatially dependent Hamiltonian, the following spinor is introduced

$$\left|\Psi_{\mathbf{k}}\right\rangle = \begin{pmatrix} \left|\Psi_{\mathbf{k_1}}\right\rangle \\ \left|\Psi_{\mathbf{k_2}}\right\rangle \end{pmatrix} := \begin{pmatrix} c^{\dagger}_{\mathbf{k},\uparrow} \\ c_{-\mathbf{k},\downarrow} \end{pmatrix} \left|\psi_{\mathrm{BCS}}\right\rangle \tag{1.16}$$

In this basis $\left\{\left|\Psi_{\mathbf{k_1}}\right\rangle, \left|\Psi_{\mathbf{k_2}}\right\rangle\right\}$, the Hamiltonian is (and this is the Bogoliubov de Gennes Hamiltonian with energies relative to $E_{\mathbf{k}}$):

$$H_{\mathrm{BdG}}\left(\mathbf{k}\right) = \begin{pmatrix} \xi_{\mathbf{k}} & -\Delta_{\mathbf{k}} \\ -\Delta^{*}_{\mathbf{k}} & -\xi_{\mathbf{k}} \end{pmatrix} \tag{1.17}$$

This Hamiltonian form eq. (1.17) has the eigenvalues

$$\pm E_{\mathbf{k}} = \pm\sqrt{\xi^2_{\mathbf{k}} + |\Delta_{\mathbf{k}}|^2}. \tag{1.18}$$

To finally arrive at the spatially dependent form of eg. (1.17), the Hamiltonian is Fourier-transformed.

$$H_{\mathrm{BdG}}\left(\mathbf{r}\right) := \frac{1}{N} \sum_{\mathbf{k}} e^{i\mathbf{k}\cdot\mathbf{r}} H_{\mathrm{BdG}}\left(\mathbf{k}\right) \tag{1.19}$$

$$= \begin{pmatrix} H_0\left(\mathbf{r}\right) & -\Delta\left(\mathbf{r}\right) \\ -\Delta^{*}\left(\mathbf{r}\right) & -H_0\left(\mathbf{r}\right) \end{pmatrix} \tag{1.20}$$

$H_0\left(\mathbf{r}\right)$ is the free Hamiltonian. Corresponding Schrödinger equaions are called BdG-equations:

$$H_{\mathrm{BdG}}\left(\mathbf{r}\right)\Psi\left(\mathbf{r}\right) = E\Psi\left(\mathbf{r}\right) \tag{1.21}$$

$$\Psi\left(\mathbf{r}\right) = \begin{pmatrix} \Psi_1\left(\mathbf{r}\right) \\ \Psi_2\left(\mathbf{r}\right) \end{pmatrix} \tag{1.22}$$

1.2 Theory of NS interface, Andreev reflection at NS interfaces

Starting with Hamiltonian in eq. (1.20), and $\Delta\left(\mathbf{r}\right) = \Delta_0\theta\left(x\right)$ and $H_0 = \frac{\hbar}{2m}\nabla^2 + \mu^2$. For some reasons, there is a sign change here... Normal region: $x < 0$, superconducting region: $x > 0$. Now: Solve the BdG-euqationg from eq. (1.21) for the two different regions.

Solution for the normal region

Normal region, components of eq. (1.22) are just superpositions of plane waves Set $\hbar = 1$ Solution to the normal side:

$$k_{1/2}^2 = k_F^2 \pm 2mE \tag{1.23}$$

Solution in the superconducting region

Energy above the gap: $|\mathbf{E}| > \boldsymbol{\Delta_0}$ Plane vectors again, wave functions from BdG equations are coupled:

$$\Psi_2(\mathbf{r}) = \frac{1}{\Delta_0}\left(E + \frac{1}{2m}\nabla^2 + \mu\right)\Psi_1(\mathbf{r}) \tag{1.24}$$

Above means, the amplitudes are coupled and the solution is given by:

$$q_{1/2}^2 = 2m\left(\mu + \sqrt{E^2 - \Delta_0^2}\right) \tag{1.25}$$

Energy below the gap: $|\mathbf{E}| < \boldsymbol{\Delta_0}$ This is where the magic happens... Ansatz:

$$\Psi_1(\mathbf{r}) = e^{i(\mathbf{k}_{1,\parallel}\cdot\mathbf{r}_\parallel)}\Phi_1(x) \tag{1.26}$$

$$\Rightarrow \left(-\frac{k_{1,\parallel}^2}{2m} + \frac{1}{2m}\frac{d^2}{dx^2} + \mu\right)^2 \Phi_1(x) = (E^2 - \Delta_0^2)\Phi_1(x) \tag{1.27}$$

Make an exponential ansatz (why this particular form?):

$$\Phi_1(x) = e^{\kappa x + iqx} \tag{1.28}$$

Plugging in ansatz leads to (by comparing real and imaginary part of the right hand and left hand side)

$$\kappa^2 = k_{1\parallel}^2 + q^2 - 2m\mu \tag{1.29}$$

$$-\frac{\kappa^2 q^2}{m} = E^2 - \Delta_0^2 \tag{1.30}$$

Next step: write down explicit solutions for q and κ:

$$q^2 = \frac{1}{2}\left(k_F^2 - k_{1,\parallel}^2 \pm \sqrt{(k_F^2 - k_{1,\parallel}^2) + 4m(\Delta_0^2 - E^2)}\right) \tag{1.31}$$

Assumption for real q makes only solution with plus sign in squareroot possible.

$$q = \pm q_1 := \pm\frac{1}{\sqrt{2}}\sqrt{\left(k_F^2 - k_{1,\parallel}^2 \pm \sqrt{(k_F^2 - k_{1,\parallel}^2) + 4m(\Delta_0^2 - E^2)}\right)} \tag{1.32}$$

Therefore we find for κ:

$$\kappa^2 = \frac{1}{2}\left(k_{1,\parallel}^2 - k_F^2 \pm \sqrt{(k_F^2 - k_{1,\parallel}^2) + 4m(\Delta_0^2 - E^2)}\right) \tag{1.33}$$

In this case, only the negative solution of κ is relevant, because the positive solution would grow exponentially for $x \to \infty$.

$$\kappa = -\kappa_1 := \pm\frac{1}{\sqrt{2}}\sqrt{\left(k_{1,\parallel}^2 - k_F^2 \pm \sqrt{(k_F^2 - k_{1,\parallel}^2) + 4m(\Delta_0^2 - E^2)}\right)} \tag{1.34}$$

Since the solutions for $\Psi_1(x)$ and $\Psi_2(x)$ are proportional to each other, we already know, that the solving the differential equation with the ansatz from ref? will lead to the same result. In other word, since $\mathbf{k_1}_{,\parallel} = \mathbf{k_2}_{,\parallel}$, it follows directly that $\kappa_1 = \kappa_2$ and $q_1 = q_2$. Plugging in the results, we find

$$\Psi_2(x) = \frac{E \mp i\sqrt{\Delta_0^2 - E^2}}{\Delta_0}\Psi_1(x) \tag{1.35}$$

Short summary: so far we have only found, how the two spinor components are related. Now we need an ansatz for the spinor to solve the BdG equation itself. (Maybe mention this one earlier, in the part for the solution in the normal region?)

$$\Psi(r) = \begin{pmatrix} e^{i\mathbf{k}_1\mathbf{r}} + r \cdot e^{i\tilde{\mathbf{k}}_1\mathbf{r}} \\ a \cdot e^{i\mathbf{k}_2\mathbf{r}} \end{pmatrix} \quad \text{for} \quad x \leq 0 \tag{1.36}$$

$$\tilde{\mathbf{k}}_1 = \begin{pmatrix} -k_{1,x} \\ k_{1,y} \\ k_{1,z} \end{pmatrix}, \quad \mathbf{k}_2 = \begin{pmatrix} k_{2,x} \\ k_{1,y} \\ k_{1,z} \end{pmatrix}, \quad k_{2,x} > 0 \tag{1.37}$$

$$k_{1,x}^2 + k_{1,\parallel}^2 = k_F^2 + 2mE \tag{1.38}$$

$$k_{2,x}^2 + k_{1,\parallel}^2 = k_F^2 - 2mE \tag{1.39}$$

Ansatz for wave function in superconducting region: two solutions for $q = \pm q_1$, $\kappa = -\kappa_1$ leads to $\Phi(x) = e^{\kappa x + iqx} = e^{-\kappa_1 x}\left(e^{+iq_1 x} + e^{-iq_1 x}\right)$

$$\Psi(\mathbf{r}) = e^{-\kappa_1 x}\begin{pmatrix} \alpha_+ e^{i(q_1 x + \mathbf{k}_\parallel \cdot \mathbf{r}_\parallel)} + \alpha_- e^{i(-q_1 x + \mathbf{k}_\parallel \cdot \mathbf{r}_\parallel)} \\ \beta_+ e^{i(q_1 x + \mathbf{k}_\parallel \cdot \mathbf{r}_\parallel)} + \beta_- e^{i(-q_1 x + \mathbf{k}_\parallel \cdot \mathbf{r}_\parallel)} \end{pmatrix} \tag{1.40}$$

1.3 Theory of SNS junction

1.4 Specular Andreev reflection, graphene specifics

2 Analytical Model

This chapter intends to explain the calculation of the critical current in different SNS junctions. For this purpose, a quasiclassical transport theory is used and its foundations are explained in the first section. This technique is then employed for a clean SNS junction, and an expression for the Josephson current is found. In the following section, the calculations used for the clean setup are extended for the more sophisticated quantum point contact (QPC) and here as well, the current for the QPC-gated junction is found.

2.1 Foundation of the quasiclassical model

This section explains preliminary assumptions made to describe the current in a SNS junction. The aim is to express the current through the junction using a quasiclassical approach. Essentially, this means that the Andreev bound states are associated with straight trajectories connecting the superconducting leads. The superconducting current density is then expressed in terms of these trajectories. The two dimensional junction, a schematic is shown in fig 2.1, is a short and wide

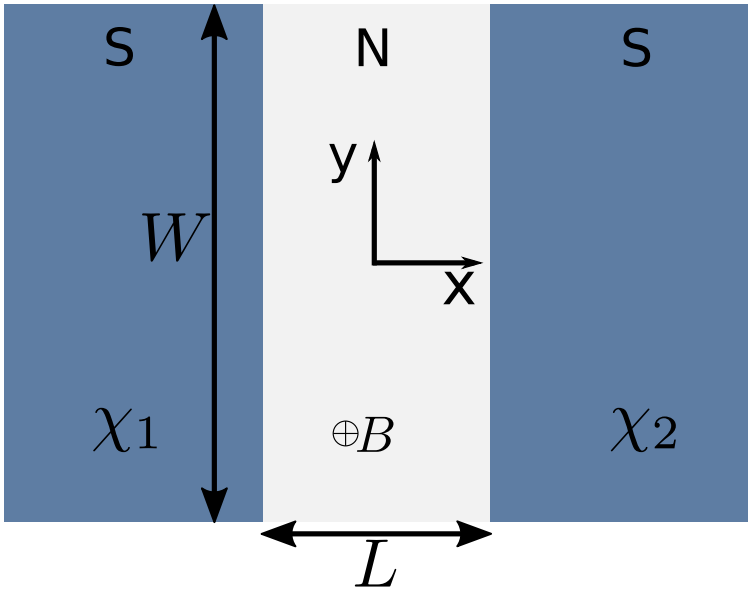

Figure 2.1: *Schematic representation of a short and wide SNS junction.*

junction with width W and length L, where $W \gg L$. The NS-interfaces are parallel to the y-axis and are placed at $x = \pm L/2$. Each of the superconducting leads has a phase χ_1 and χ_2, and

the overall phase difference is $\chi = \chi_1 - \chi_2$. The superconducting gap parameter is only present in the superconducting leads. Close to the interface, Δ begins to decay on a length scale of the superconducting coherence length ξ_0 into the normal region. For the following calculations, this effect is neglected and a step-like behavior is assumed for the superconducting gap parameter.

$$\Delta(x) = |\Delta| e^{\chi_1} \Theta\left(-L/2 - x\right) + |\Delta| e^{\chi_2} \Theta\left(x - L/2\right) \tag{2.1}$$

We consider the low temperature limit, where the thermal length scale of the system is larger than the sample length:

$$L_T = \hbar v_F / k_B T \gg L \tag{2.2}$$

The considered sample is ballistic, which means the fermi wavelength λ_F is smaller than the sample length L. It has the BCS coherence length $\xi = \hbar v_F / \pi \Delta$, where ξ is much larger than the Fermi velocity $\xi \gg v_F$ **TODO: (in order to induce superconductivity in the system?)**. The relation between the coherence length ξ and the sample length L determines if the considered junction is a *short* or a *long* junction:

$$\begin{aligned} \xi \ll L \quad &\rightarrow \quad \text{long junction} \quad \rightarrow \quad \text{many Andreev levels} \\ \xi \gg L \quad &\rightarrow \quad \text{short junction} \quad \rightarrow \quad \text{one Andreev level} \end{aligned}$$

TODO: replace equation above with good picture (E ¡ delta, andreec levels...)
TODO stimmt das oben? Es sollte einen Zusammenhang primaer mit Energie, nicht mit sample size geben... The presence of the magnetic field in the normal region of the sample will lead to a bending of the trajectories due to the Lorentz force. Depending on the strength of magnetic field B and the Fermi velocity, the radius of this curve is

$$r_B = \frac{m^* v_F}{eB} \tag{2.3}$$

In order to justify the assumption of straight trajectories, either the magnetic field has to be weak enough, or the Fermi velocity (wavelength) has to be large (short) enough. Then, the cyclotron radius r_B is larger than the sample size L and the ass straight trajectories are a valid assumption.

2.2 Plane setup: calculation of current

To derive the current for the SNS setup depicted in figure 2.1, we start by writing down the Bogoliubov-de-Gennes Hamiltonian for this system.

$$\begin{pmatrix} -\frac{\hbar^2}{2m}\nabla^2 - \epsilon_F & \Delta(x) \\ \Delta^*(x) & \frac{\hbar^2}{2m}\nabla^2 + \epsilon_F \end{pmatrix} \begin{pmatrix} \psi_e \\ \psi_h \end{pmatrix} = E \begin{pmatrix} \psi_e \\ \psi_h \end{pmatrix} \tag{2.4}$$

The Hamiltonian above uses eq. (2.1) for the spatially dependent superconducting gap parameter $\Delta(x)$. The eigenvalue problem has two solutions

$$\epsilon_\pm = \frac{\hbar^2 k_\pm^2}{2m} = -\epsilon_F - \sqrt{E_k^2 - |\Delta|^2} \tag{2.5}$$

TODO: Hier fehlt die Herleitung für Wellenfunktionen, Ausdruck für den Strom etc.!
Current density for short and long junction limit: In the short junction limit the current density can be derived from the scattering matrix formalism and it reads

$$\mathcal{J}^s(\chi) = \frac{\mathcal{T} \sin\chi}{\sqrt{1 - \mathcal{T} \sin^2 \frac{\chi}{2}}} \tag{2.6}$$

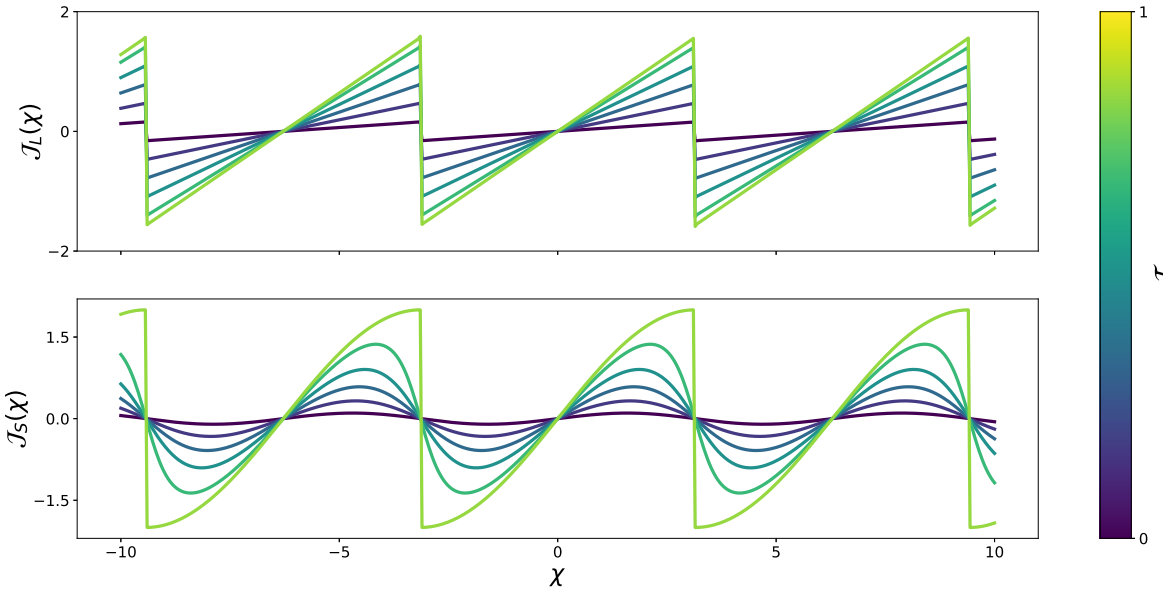

Figure 2.2: *Short and long junction current density*

$\mathcal{T}$ is the transmission coefficient that describes the transmission through a channel (each channel corresponds to a eigenvalue of the scattering matrix. The current density for the long junction limit is

$$\mathcal{J}(\chi) = \sum_{k=1}^{\infty} \frac{(-1)^{k+1}}{k} \sin\big(k\chi\big). \tag{2.7}$$

Figure 2.2 shows a plot of both short and long junction limit current densities. They differ for a large transmission coefficient $\mathcal{T} \simeq 1$, where in the long junction limit we observe a sawtooth like shape and in the short junction limit we have a sinusoidal shape.
A trajectory connecting the superconducting interfaces can be parametrized by

$$\tan\theta = \frac{y_2 - y_1}{L} \tag{2.8}$$

with θ being the angle between the trajectory and the x-axis.
TODO: figure!
Using the current density the Josephson current at zero magnetic field ($\phi = 0$) can be expressed as

$$J\left(\chi, \phi = 0\right) = \frac{2ev_F}{\pi\lambda_F L^2} \int \int_{-W/2}^{W/2} dy_1 dy_2 \frac{\mathcal{J}(\chi)}{\left[1 + \left(\frac{y_1 - y_2}{L}\right)^2\right]^2} \tag{2.9}$$

Including magnetic field

Include parametrizaation of trajectories somewhere, important for calculation of magnetic phase!
So far, the current has been derived for zero magnetic field. If a finite magnetic field is considered, the phase χ will be modified because of two effects. The magnetic phase that will be acquired

along a trajectory connecting two points y_1 and y_2 leads to an additional term in the phase. Then again, *the condition of zero screening current in the bulk superconducting region and the limit of* $\lambda_L \to 0$ *require the superconducting phase at the interfaces to become functions of y.*
TODO: Umschreiben!

$$\chi_{1/2} = \mp\frac{1}{2}\left(\chi - \frac{2\pi BL}{\phi_0} y_{1/2}\right) \tag{2.10}$$

$$\tilde{\chi}(y_1, y_2) = \chi_2 - \chi_1 \tag{2.11}$$

$$= \chi - \frac{\pi BL}{\phi_0}(y_1 + y_2) \tag{2.12}$$

Assuming that the London penetration depth is small to zero in the superconducting regions the following gauge for the vector potential can be used

$$\mathbf{A} = A_y \mathbf{e}_y, \quad A_y = \begin{cases} -Bx, & -L/2 \le x \le L/2, \\ -\frac{1}{2}BL|x|, & |x| > L/2 \end{cases} \tag{2.13}$$

This gauge will give no additional contribution to the phase on straight trajectories

$$\delta\chi = \frac{2\pi}{\Phi_0}\int d\mathbf{l}\cdot\mathbf{A} \tag{2.14}$$

$$= \frac{2\pi}{\Phi_0}\int_{-L/2}^{L/2}\frac{dx}{\cos\theta}A_y(x)\sin\theta \tag{2.15}$$

$$= -\frac{2\pi B}{\Phi_0}\frac{y_2 - y_1}{L}\int_{-L/2}^{L/2} x dx \tag{2.16}$$

$$= 0, \tag{2.17}$$

where eq (2.8) has been used. The total phase for this setup therefore is eq. (2.12). This mean that the current phase relation in the expression for the Josephson current from eq. (2.9) for zero magnetic field has to replaced by the effective phase $\chi \to \tilde{\chi}(y_1, y_2)$ and then reads

$$J\left(\chi, \phi\right) = \frac{2ev_F}{\pi\lambda_F L^2}\int\int_{-W/2}^{W/2} dy_1 dy_2 \frac{\mathcal{J}(\tilde{\chi}(y_1, y_2))}{\left[1 + \left(\frac{y_1 - y_2}{L}\right)^2\right]^2} \tag{2.18}$$

By maximizing the Josephson current with respect to χ, the critical current can be found:

$$I_c(\phi) = \max_\chi\left\{J(\chi, \phi)\right\} \tag{2.19}$$

TODO: Dependence on W/L ratio? Plot of current?

2.3 Calculation of QPC current

TODO: what happens when a constriction is on top of normal layer, fermi levels etc
The quasiclassical formalism can even be employed to modified SNS junctions. One can build gates on top of the normal region of the junction in a way that the current cannot pass through the gated regions. In the quasiclassical picture, this means that the possibilites for trajectories connecting two points at the superconducting interfaces are limited through the geometry of the

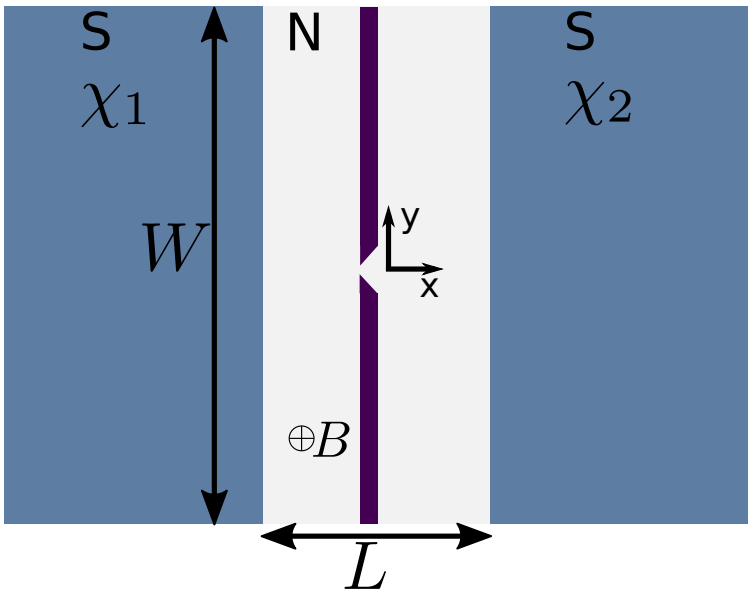

Figure 2.3: *QPC setup.*

constriction.
Figure 2.3 shows a sketch of the quantum point contact setup which will be analysed with the quasiclassical formalism. The normal region of the SNS junction is covered by a gate with a small split in the middle. The split is located at $(xy) = (0, 0)$ so that the sample is symmetric around the origin. The width of the split is in the order of λ_F (**Warum wichtig?**) and can thereby be modeled as an isotropic scattering point with transmission coefficient $\mathcal{T}_0$. Trajectories connecting the two superconducting interfaces have therefore to pass through the QPC. For simplicity the geometrical width of the barrier is neglected and only straight trajectories are considered and scattering at side edges is neglected. This modified setup leads first to a different parametrization of the trajectories and therefore to a different magnetic phase than in eq. (**??**).
With the QPC setup, all possible trajectories are parametrized by two angles θ_1 and θ_2. θ_1 describes the trajectory before passing through the QPC in the region $-L/2 < x0$ and θ_2 after passing through the QPC. The parametrization of the trajectories reads

$$\tan\theta_1 = -\frac{2y_1}{L}, \quad \tan\theta_2 = \frac{2y_2}{L} \tag{2.20}$$

With the gauge from eq. (2.13) the magnetic phase acquired within the sample reads

$$\frac{2\pi}{\Phi_0}\int d\mathbf{l}\cdot\mathbf{A} \;=\; -\frac{\pi B}{\Phi_0}\left(\frac{L}{2}\right)^2\left(-\tan\theta_1+\tan\theta_2\right) = -\frac{\pi\phi(y_1+y_2)}{2W}. \tag{2.21}$$

Adding this contribution to the term in eq. (2.12) the effective phase for the QPC setup is found

$$\tilde{\chi}(y_1, y_2) = \chi - \frac{3\pi\phi}{2W}(y_1+y_2). \tag{2.22}$$

The contribution in eq. (2.22) is half of the effective phase without any constriction, as written in eq. (2.12). This is reasonable and can be illustrated by looking at the area contributing to the phase. Only half of the normal region is covered by all possible trajectories in the QPC case, whereas in the case without any constriction, the whole normal region contributes.
TODO: stimmt das da oben? warum?

One consequence of the additional gate on top of the normal region is the change in the effective phase and consequently a modified current phase relation $\mathcal{J}(\tilde{\chi}(y_1, y_2)$. Another consequence is a modified expression for the critical current. In the setup without gates, straight trajectories with a fixed angle θ were considered and summed up to a total contribution. The difference in the QPC setup is the split in the gate, which is modeled as an isotropic scattering point. The trajectories being summed up in this setup can be thought of two parts. The first part connects y_1 with the split at $(x, y) = (0, 0)$ and is determined by the direction of the trajectory. This is why the Fermi velocity enters in this part. The second part of the current trajectory starts from the origin and connects it with a point at the right interface y_2. To sum up, the critical current in the QPC setup is

$$I_c^{\mathrm{QPC}}(\phi) \propto \max_\chi \int d\theta_1 v_F \cos^2\theta_1 \int d\theta_f \cos\theta_f \mathcal{J}\left(\tilde{\chi}(\theta_1, \theta_2)\right) \tag{2.23}$$

The QPC is modeled as an isotropic scatterer with transmission probability $\mathcal{T}$. If the transmission is small, $\mathcal{T} << 1$, eq. (**TODO: add reference and add formula**) can be used for $\mathcal{J}$. **TODO: add why from** $\sin\tilde{\chi}$ **only cosine survives!** The angles $\theta_{1,2}$ can be rewritten in terms of $y_{1,2}$ by using the parametrization from eq. (2.20). Using this, the normalized critical current can be expressed as

$$\frac{I_c(\phi)}{I_c(0)} = \frac{\mathcal{I}_2(\phi)\mathcal{I}_{3/2}(\phi)}{\mathcal{I}_2(0)\mathcal{I}_{3/2}(0)}, \tag{2.24}$$

where the integrals $\mathcal{I}$ are defined as

$$\mathcal{I}_k(\phi) = \frac{2}{L}\int_{-W/2}^{+W/2} dy \frac{\cos\left(\frac{3\pi\phi y}{2W}\right)}{\left[1 + \left(\frac{2y}{L}\right)^2\right]^k} \tag{2.25}$$

The current can be evaluated in the limit of small flux $\phi \to 0$ and in limit of high fields $\phi \to \infty$. At $\phi = 0$ the cosine term becomes one leading to the simple expression

$$\mathcal{I}_2(0)\mathcal{I}_{3/2}(0) = \frac{2W}{\sqrt{L^2+W^2}} \arctan\frac{W}{L} + \frac{2LW^2}{(L^2+W^2)^{3/2}} \tag{2.26}$$

$$\equiv \frac{2x}{\sqrt{1+x^2}} \arctan x + \frac{2x^2}{\left(1+x^2\right)^{3/2}}, \quad x = W/L \tag{2.27}$$

The parabolic asymptotics of the critical current at small ϕ is found by expanding the cosine factors in the numerator:

$$\frac{I_c(\phi)}{I_{c0}} \simeq 1 - \frac{9\pi^2\phi^2}{32} f_0(W/L) \tag{2.28}$$

$$f_0(x) = \frac{\sqrt{x^2+1}\log\left(\sqrt{x^2+1}+x\right)}{x^3} - \frac{2}{x(x+(x^2+1)\arctan x)} \tag{2.29}$$

In the opposite limit of high fields, $\phi \to \infty$, we extend the integration in Eq. (2.25) over y_1 and y_2 to $\pm\infty$ and obtain

$$\frac{I_c(\phi)}{I_{c0}} = \frac{\pi^2\left(1+x^2\right)^{3/2}}{4x\left(x+\left(1+x^2\right)\arctan x\right)}\left(1+\frac{3\pi\phi}{4x}\right)\sqrt{\frac{3\phi}{2x}}\exp\left(-\frac{3\phi\pi}{2x}\right) \tag{2.30}$$

TODO: write this one in pretty

2.4 QPC edge current

Quasiclassical model applied to edge currents. Parametriztion here:

$$\tan\theta_1 = \frac{W-y_1}{L/2}, \quad \tan\theta_2 = -\frac{W-y_2}{L/2} \tag{2.31}$$

Magnetic phase gain along trajectory:

$$\begin{aligned}
\frac{2\pi}{\phi_0}\int d\mathbf{l}\cdot\mathbf{A} &= \frac{2\pi}{\phi_0}\left(\int A_y(x)|d\mathbf{l}||\mathbf{e_y}|\sin\theta_1 + \int A_y(x)|d\mathbf{l}||\mathbf{e_y}|\sin\theta_2\right) && (2.32)\\
&= -\frac{2\pi B}{\phi_0}\left(\int_{-L/2}^{0} x dx\tan\theta_1 + \int_0^{L/2} x dx\tan\theta_2\right) && (2.33)\\
&= -\frac{\pi B}{\phi_0}\frac{L}{2}\left(-\tan\theta_1+\tan\theta_2\right) && (2.34)\\
&= -\frac{\pi B}{\phi_0}\frac{L}{2}\left(-2W+(y_1+y_2)\right) && (2.35)\\
&= \pi\Phi - \frac{\pi\Phi}{2W}(y_1+y_2) && (2.36)
\end{aligned}$$

Using

$$\Phi = \frac{\phi}{\phi_0}, \quad \phi = BWL \tag{2.37}$$

Remember contribution from setup without any constriction eq. (2.12), adding this up leads to a total phase for the edge transmission

$$\tilde{\chi}(y_1,y_2) = \chi - \frac{3\pi\Phi}{2\phi_0}(y_1+y_2) + \pi\Phi \tag{2.38}$$

Bibliography

[1] J. Bardeen, L. N. Cooper and J. R. Schrieffer. Theory of Superconductivity. *Physical Review*, 108(5):1175–1204, dec 1957.